Al-Azhar Bulletin of Science, Section A, Vol. 33, No. 1 (June) 2022, pp. 27-39
http://doi.10.21608/absb.2022.115408.1166

Al-Azhar Bulletin of Science: Section A

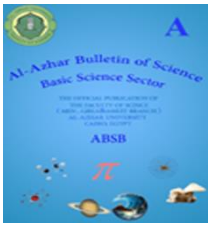

HEAVY METAL IONS AND FLUORIDE REMOVAL FROM WASTEWATER USING MORINGA SEED BEADS

Khalid M. Khader [a,*], Rabie S. Farag [a], Moustafa M.S. Abo-Elfadl [b], Mohamed E.A. Ali [b]

[a] Department of Chemistry, Faculty of Science (Boys), Al-Azhar University, Cairo, Egypt.
[b] Desert Research Center, Cairo, Egypt.

*Corresponding author: khalidkhedr49@gmail.com

Received: 17 Jan 2022; Revised: 16 Feb 2022; Accepted: 17 Feb 2022; Published: 01 Jun 2022

ABSTRACT

Water contamination by heavy metals has harmful and hazardous health consequences for humans. The goal of this study is to see how effective Moringa seeds beads (MOSB) mixed with sodium alginate are at adsorbing ions like copper, nickel, manganese, lead and fluoride from polluted water. Different instrumental approaches were used to characterize the adsorbent (FT-IR and SEM). Batch adsorption studies and the effects of the adsorption parameters were optimized. The results revealed that the removal rate for each element occurred at the optimum dose (5g/l) with removal efficiency (93, 72, 80, 96, and 93 %) and the maximum sorption capacity ($Q_{max.}$) of about (12.5, 8, 8.3, 13, and 13 mg/g) for copper, nickel, manganese, lead and fluoride ions, respectively. The pH, coagulant dosage, mixing, concentration, and the initial turbidity of the water all had an impact on the removal of heavy metals and fluoride ions. MOSB can be considered as sustainable alternative material because it is inexpensive, requires no prior treatment, and it is a bio-sorbent for removal of heavy metals and fluoride ions from wastewater.

Keywords: Moringa seeds beads; Heavy metal removal; Adsorption isotherms; Reusability.

1. INTRODUCTION

Every living species requires water in order to survive. Contaminated water supply must be treated because it can be used for human consumption. Heavy metals have the tendency to build up in the human body, making them poisonous and dangerous [1]. Some metals, including copper, zinc, nickel, and chromium, are essential for cellular metabolism but can be hazardous at excessive doses. Other metals, such as lead and cadmium, are harmful even at trace quantities [2]. Aqueous toxic waste from a variety of activities, such as metal plating, logging, tanning, "etc.", causes heavy metal contamination [3].

Adsorption methods using economical adsorbent materials are used in several different ways for heavy metal removal from polluted water [4, 5]. Heavy metals were removed using bio-sorbents such as sugarcane bagasse [5, 6], mussel shells [7], and dry biomass of Eichornia crassipes [2]. Agricultural wastes such as fly ash, bagasse and peat can be employed as heavy metal bio-sorbents [8]. In addition, corn cobs, rice husks and straws [9], soya beans, sawdust, walnut and cotton seed hulls, and banana peels [10] are good examples of alternative bio-sorbents. Low-cost adsorbents have demonstrated excellent pollution removal capacities. Cheap adsorbents can be modified to

change their original qualities, making them ideal for sorting a variety of waste items.

The grinding seeds of the Moringa oleifera plant contain coagulating qualities that have been used to reduce turbidity, alkalinity, total dissolved solids, and hardness in water [11, 12]. However, it has received insufficient attention for its biosorption behaviour in the removal of hazardous metals from water bodies [13]. MOSB (Moringa seed beads) were employed as an adsorbent to remove ions from an aqueous solution [14]. To increase the adsorption ability of MOSB, it was chemically activated with citric acid. Moringa oleifera press cake was used to remove (Fe, Cu, and Cr) from wastewater [15]. Aziz et al. [16, 17] demonstrate that moringa seeds, banana peel, and their mixture have the potential to be utilized as a natural alternative to the other water treatment agents for elimination Pb, Ni, and Cd from drinking water.

The present work aimed to study the use of calcium alginate beads of de-oiled Moringa Oliefera Seeds (MOS) as natural bio-sorbent to determine their efficiency to reduce metal ions such as (Cu^{2+}, Ni^{2+}, Mn^{2+} and Pb^{2+}), and F^- in synthetic water. Their effectiveness was evaluated at different parameters to find the best operating conditions for maximum metal ions removal in a water treatment plant.

2. EXPERIMENTAL

2.1. Preparation of the residual cake of Moringa olifera seeds (MOS).

The MOS were cultivated from a local farm at Abo-Hammad, Sharkiaa, Egypt. The husks were pilled-off, and then the seeds were grounded and were sieved through 500, 180 and 75μm sieves. The seeds were rinsed in de-ionized water to remove dust, then immersed in 1 M HCl for 3 days, to remove heavy metals content. Then treated with 1.0 M NaOH soln. The seeds were again rinsed in distilled water and dried in air drier then grounded using a pestle and mortar. De-fating was carried out using hexane as an organic solvent for 12 hours, then centrifuged many times until no more fat remained in the biomass. The wet MOS powder was then dried in an oven at 50 °C for 72 h after which it was grinded again and sieved through 75 um and 25 um sieves.

2.2. Moringa seeds beads formation (MOSB).

The MOSB were de-shelled and rinsed with de-ionized water, air-dried, and the pulverization process was carried out to get a fine powder, which was encapsulated by cross-link polymerization of sodium alginate and calcium chloride. The grinding alginate was dissolved in a phosphate-buffered saline solution to generate a viscous solution with varied concentrations (ranging from 1–3 %) to improve the characteristics of the beads. With the help of a peristaltic pump, they are allowed to fall drop by drop into a sterile calcium chloride solution (3 %, w/v). The flow rate of the pump was set to 250 spherical beads per hour. Following encapsulation, the beads in the salt solution were incubated at room temperature for 2 h for the complete replacement of ions and then beads were stored at 4 °C.

2.3. Characterization

The IR analysis of Moringa seeds and its beads were analyzed with FTIR spectrophotometer (Shimadzu FTIR-8400, Japan). A scanning electron microscope (type JEOL JSM-6360, Japan) was used to examine the surfaces' morphology.

2.4. Batch adsorption studies

Batch studies were undertaken to determine the best experimental conditions, which included contact time (15 to 250 minutes), adsorbent dosage (1–5 g), and pH (2–8). Tests were carried out in 100 ml beakers to study the effect of parameters (pH values, adsorbent weight and contact time). The beakers were shaken for a prescribed length of time by magnetic stirrer at room temperature. After filtration (Whatman 42mm), the remaining concentration of Cu^{2+}, Ni^{2+}, Mn^{2+}, $Pb^{2+}$and F^- ions was measured by AAS. The amount of the metal adsorbed (% removal) by the sorbent was calculated using Eqn. 1.

$$\% \text{ Removal Efficiency} = ((C_i - C_f)/C_i) \times 100$$ Eqn. 1

The amount of adsorbed metal ions onto the surface of the adsorbent was calculated from the mass balance expression given by Eqn. 2:

$$q_e = \frac{(C_i - C_f)}{M} V$$ Eqn. 2

Where, q_e is the amount of metal ions adsorbed (mg/g); C_i, initial metal ion concentration (mg/L), C_f is the final metal ion concentration (mg/L), M is the mass of the adsorbent in (g), and V is the volume (liter) of the metal solution in contact with the adsorbent.

2.5. Adsorption isotherms

To match the experimental results and understand the adsorption mechanism of Cu^{2+}, Ni^{2+}, Mn^{2+}, Pb^{2+} and F^- onto the surface of MOSB as adsorbent mater, The adsorption isotherm models of Langmuir and Freundlich were used For Langmuir model the linear form could be expressed by the following equation:

$$C_e/ q_e = 1/ KLq_{max} + C_e/ q_{max}$$ Eqn. 3

The Freundlich model, the linear form could be expressed from the following equation:

$$\text{Log } q_e = \log k_F + (1/n) \log C_e$$ Eqn. 4

Where C_e is the equilibrium concentration of metal in mg/l, q_e and q_m are the adsorped amount at equilibrium (mg/g) and adsorption capacity (mg/g), respectively, and K_L is the Langmuir constant (L/mg). The values of K_L and q_m can be obtained from the intercept and slope of C_e/q_e versus C_e. K_F is the empirical Freundlich constant (mg/g) and 1/n is the Freundlich exponent.

To predict whether an adsorption system is favorable or unfavorable, the equilibrium parameter (R_L) was calculated according to the following equation 5:

$$R_L = \frac{1}{1 + bC_e}$$ Eqn. 5

Where b is the Langmuir constant (l/mg) and C_f is the final concentration (mg/l) in the solution, if $R_L > 1$ the isotherm is unfavorable, whereas if $R_L < 1$ the isotherm is favorable.

The linear form of the Langmuir model [19] and Freundlich model [Freundlich (1906)] can be stated.

The equilibrium parameter (R_L) was calculated to predict the adsorption system is favourable or unfavourable.

2.6. Adsorption Kinetics

To match the experimental results and understand the adsorption mechanism of Cu^{2+}, Ni^{2+}, Mn^{2+}, Pb^{2+} and F^- onto the surface of MOSB as adsorbent mater, the pseudo-first-order kinetic model [20] and pseudo-second-order kinetic model [21] were used.

The pseudo-first-order kinetic model and pseudo-second- order kinetic model, were employed to fit the experimental data and to understand the adsorption mechanism of Cu^{+2},Ni^{+2}, Mn^{+2},Pb^{+2}, and F^- ions onto the surface of MOSB as adsorbent matter. The equation of Pseudo-first-order kinetic model is as follows:

$$\log (q_e - q_t) = \log q_e - ((k_1/2.303) * t)$$ Eqn. 6

where q_t and q_e (mg /g) are the amounts of metal ions adsorbed per unit mass of the adsorbent at time t (min) and equilibrium, respectively, and k_1 (1/min) is the pseudo-first-order rate constant of the sorption process. The equation of Pseudo-second-order kinetic model is as follows:

$$t/q_t = 1/ k_2q_e^2 + t/ q_e$$ Eqn. 7

Where k_2 [g/ (mg min)] is the pseudo-second-order rate constant.

3. RESULTS AND DISCUSSION

3.1. Characterization of the bio-sorbent martial

3.1.1. Scanning electron microscopy (SEM) of bio-sorbent

Figure 1 shows many cracks and represents the presence of asymmetric pores and an open pore structure, which provides a high internal surface area on the surface of MOSB, which is favorable for bio-sorption. The pure de-oiled Moringa (MO) and Moringa powder combined

with sodium alginate (SA) exhibited a porous surface texture. Furthermore, the interaction between the MO and Sodium Alginate (SA) could have resulted in the production of a fibrous texture on the surface of the MO biomass, whereas when the SA was loaded, the surface structure became more porous, rough, and sponge-like.

3.1.2. Fourier Transform Infrared spectroscopy spectrum (FTIR)

The IR spectra of MO seeds are shown in Figure 2(A-C), with substantial peaks in the range of 3400 cm^{-1} to 800 cm^{-1}. From Fig. 2, the de-oiled MO seeds peaks appeared at 2900 cm^{-1}, 2800 cm^{-1}, 1750 cm^{-1}, 1240 cm^{-1}, and 1059 cm^{-1} are characterized by NH2, C-H symmetric stretch of alkanes, carboxyl, N-H stretch of amines, and C-O stretch of ether groups, respectively. A large band centred on the N-H stretch of secondary amines also adds to this region due to the high protein content in the seeds. The C-H asymmetric and symmetric stretch of alkanes are ascribed to the strong and high intensity peaks of MOSB, which emerged at 2926 cm^{-1} and 2856 cm^{-1}, respectively. The C=O stretch of carbonyl groups in esters and amide are attributed to the peaks at 1748 cm^{-1} and 1656 cm^{-1}, respectively, whereas the C-O stretch of ethers is assigned to the peak at 1059 cm^{-1}. Weak to medium peaks are seen at 1550 cm^{-1} (N-H bend of primary amines and amides), 1467 cm^{-1} (C-H bend of alkanes), 1243 cm^{-1} (C-O stretch of carboxylic acids and C-N stretch of amines), 1166 cm^{-1} (C-N stretch of amines) and 800 cm^{-1} (N-H wag of amines). These results indicated that the MOS is made up of a variety of functional groups, the majority of which are derived from proteins, and that they may play a crucial role in the adsorption of pollutants from polluted water. [22-24].

When SA was blended with MO, the transmittance intensities changed noticeably and were identified at 1656 cm-1 (C=O stretch of carbonyl amides), 1550 cm^{-1} (N-H bend of primary amines and amides), and 1059 cm^{-1} (C-O stretch of ethers). The removal of heavy metal

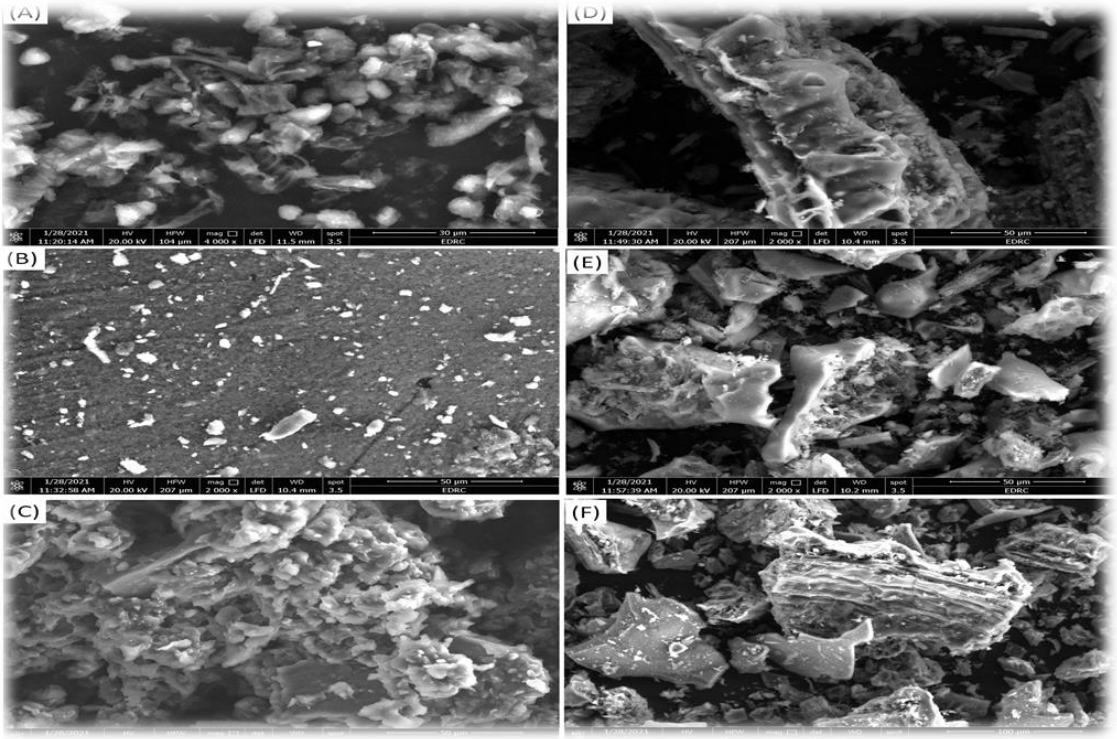

Fig. (1). The surface morphology of MO (A), SA (B), and MOSB (C).

ions and turbidity molecules from contaminated water may involve certain functional groups such as C=O stretch of carbonyl amides, N-H bend of primary amines and amides, C-O stretch of ethers, and N-H wag of amines. These groups have been shown to be capable of adsorbing heavy metals (Cu^{2+}, Mn^{2+}, Ni^{2+}, and Pb^{2+}). [25].

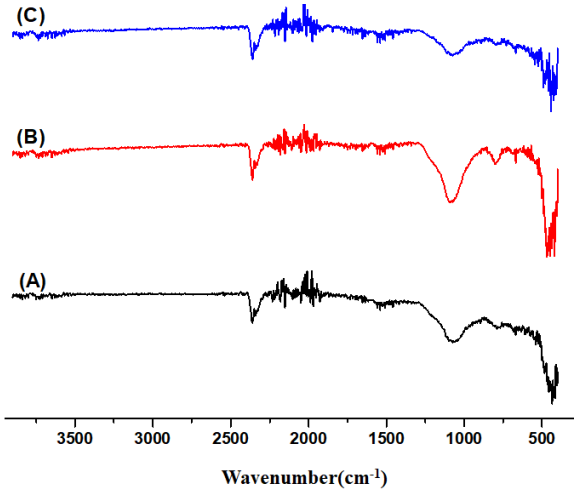

Fig. (2). FTIR spectra for (A) de-oiled MO seeds, (B) MOSB and (C) sodium alginate beads.

3.2. Factors affecting bio-sorption process of MOSB to remove metal ions such as (Cu^{2+}, Ni^{2+}, Mn^{2+}, pb^{2+}, and F^-).

3.2.1. Effect of adsorbent dose

Fig (3), illustrates the effect of the bio-sorbent doses of MOSB on bio-sorption process of metal ions for maximum metal ion removal (1-5 g/l) at constant pH (5-5.5 for metal ions) (2 for F^-)} and mixing rate 160 rpm for 90 min. It was shown that the increases of bio-sorbent dose of MOSB the increase of metal ions removal due to amino and carboxylic groups in MOSB surface are strongly reactive with metal ions particles carrying positive charges. A chelation mechanism is responsible for the absorption of metal cations by amine and carboxylic groups [26, 27]. Therefore; the optimum dose of MOSB for maximum metal ions removal occurred at constant dose (5 g/l) with removal efficiency of 93,72,80,96,93 % for Cu^{2+}, Ni^{2+}, Mn^{2+}, Pb^{2+} and F^- to MOSB, respectively. The surface area that can be employed for sorption would rise when the adsorbent dose was raised.

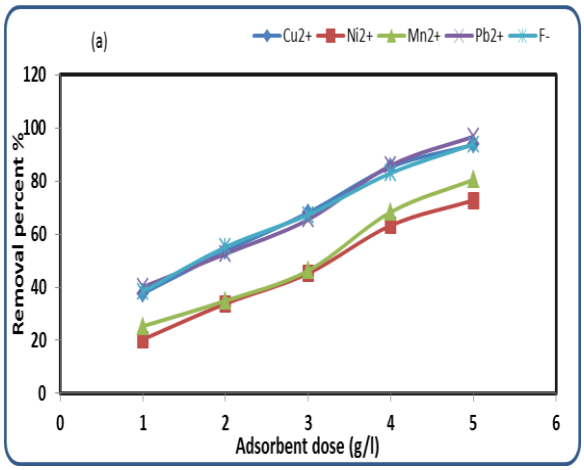

Fig. (3). Effect of adsorbent dose of MOSB on metal ions removal (Cu^{+2}, Ni^{+2}, Mn^{+2}, pb^{+2}) and F^-, at $C_\circ$= 50 mg/L, T= 25°C, t= 60 min and pH 5-5.5 for metal ions and pH 2 for F^-).

3.2.2. Effect of solution pH

Fig. (4) illustrates the percentage removal of the heavy metals (Cu^{2+}, Ni^{2+}, Mn^{2+} and Pb^{2+}) increased as the pH of aqueous solution increases. At a lower pH less than 5, the surface of the MOSB as adsorbent becomes highly protonated and hence the adsorption decreases. The degree of protonation of the surface decreases as the pH of the aqueous solution rises, and therefore the adsorption rises [28].

As shown in Fig. (4), the optimum pH for maximum metal ions and fluoride removal using beads of MOSB as adsorbent was found ranging from (5-5.5) for metal ions and pH 2 for fluoride with removal efficiency (93, 72, 80, 96 and 93) for (Cu^{2+}, Ni^{2+}, Mn^{2+} and Pb^{2+}) and F^- by MOSB respectively. This is due to, at optimum conditions and constant pH (5-5.5), an electrostatic repulsion proton of amino, carboxylic groups in MOSB is very low, so more active sites are available, hence no steric hindrance occur, and electrostatic attraction increases, so the adsorption process increases, and the removal process occur and the residual metals ion lower than the permissible limit.

In case of using MOSB as bio-sorbent for fluoride ions, the most predominated species of surface at this pH value (2-4) are positively charged that are very effective to adsorb fluoride ions [29]. As shown in Fig. (4), the optimum pH for maximum F^- ions removal

using MOSB as bio-sorbent was found ranging from (2-4) with removal efficiency ranging (93-95%), this is due decreases pH too large the medium become more acidic, the amino and carboxylic groups are highly positively charged, and the electrostatic attraction to fluoride ions increases, so the fluoride adsorption also increases.

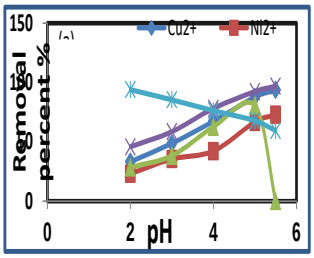

Fig. (4). Effect of varying pH of solution on adsorption process of MOSB for maximum metal ions and fluoride removal at constant dose 5 g/l

3.2.3. Effect of metal ions concentration

The elimination percent of specific heavy metal ions rose as the initial concentration (C_o) of heavy metal ions and fluoride was raised up to 50 ppm, as shown in Fig (5). This due to the fact that the initial concentration of heavy metal ions limited the removal capacity, whereas the adsorbent media contained a finite number of active sites that would have been saturated at a specific concentration. As a result, more heavy metal ion molecules competed for accessible function groups on the adsorbent material's surface. For the MOSB as adsorbent material, the highest percentage removal was occurred at constant initial concentration 50 ppm, at optimum conditions with removal efficiency (93, 72, 80, 96 and 93%) for (Cu^{2+}, Ni^{2+}, Mn^{2+}, pb^{2+} and F^-) on the surface of MOSB, respectively.

3.2.4. Effect of Contact time

Fig. (6) showed that the optimum contact time for maximum metal ions and fluoride removal was found at 90 min for both adsorbent materials. This is due to that the adsorption process was very high, due increase contact time of mixing rate led to increase the collision between the bio-sorbent molecules and metal ion and fluoride molecules, hence more active sites are available, and so, adsorption process was increased. Fig (6) indicated that, the optimum contact time at mixing rate 160 rpm for maximum metal ions and fluoride removal occurred at 90min at optimum conditions with removal efficiency (93, 72, 80, 96, and 93 %) for (Cu^{2+}, Ni^{2+}, Mn^{2+}, pb^{2+} and F^-) on MOSB respectively.

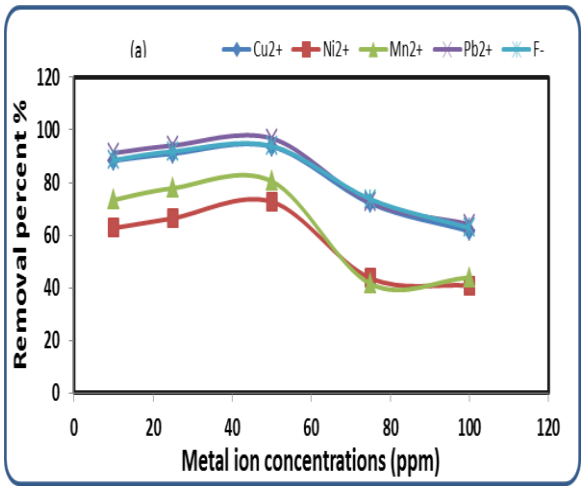

Fig. (5). Concentration effect of MOSB for maximum metal ions and fluoride removal @ T= 25°C, dose = 5 g/l, t = 60 min and (pH 5-5.5 for metal ions and pH=2 for F^-).

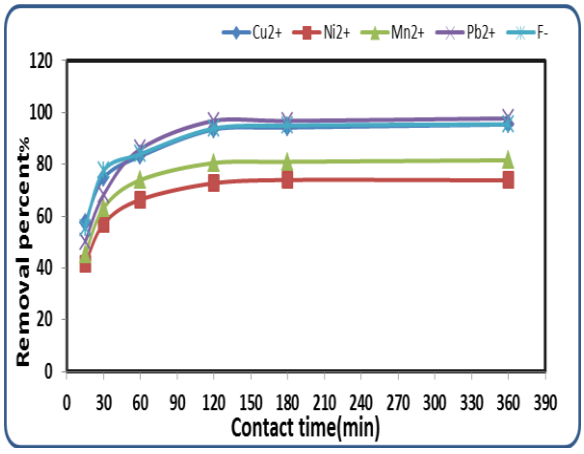

Fig. (6). Contact time effect of MOSB for maximum metal ions and fluoride removal at (T= 25°C, dose = 5 g/l, t = 60 min and (pH 5-5.5 for metal ions and pH=2 for F^-).

3.3. Adsorption Isotherms

The adsorption capacity of MOSB adsorbent to initial ion concentrations was shown in Figs. [(7a, b) to (11a, b)], where the adsorption capacity rose as the initial ion concentration increased while the removal efficiency reduced. By comparing the correlation coefficients of the two isotherm models, it was found that all R^2 values of Langmuir isotherm model (0.9963,0.976, 0.935, 0.992, 0.996) fitted better than all R^2 values of Freundlich isotherm model (0.847, 0.860, 0.708, 0.825, 0.847) corresponding to (Cu^{2+}, Ni^{2+}, Mn^{2+}, pb^{2+} and F^{-1}) respectively. This suggesting that sorption of (Cu^{2+}, Ni^{2+}, Mn^{2+}, pb^{2+} and F^{-1}) ions onto MOSB adsorbent, are monolayer coverage. This could be due to the homogeneous distribution of the multi-functional amino, carbonyl and carboxylic groups onto the surface of MOSB. The calculated maximum adsorption capacity from Langmuir isotherm model (Q_{max} = 12.59, 8.19, 8.37, 12.91 and 12.98 mg/g) for Cu^{2+}, Ni^{2+}, Mn^{2+}, pb^{2+} and F^- ions onto MOSB adsorbent respectively. From Table 1, it was illustrated that MOSB adsorbent has highest maximum adsorption capacity compared to other adsorbents. This is due to containing the adsorbent onto multi-functional groups of MOSB (amino, carbonyl and carboxylic groups), which act as chelation sites for all contaminant in polluted water.

Table 1. Illustrates the Langmuir and Freundlich isotherm models for the adsorption of Cu^{+2}, Ni^{+2}, Mn^{+2}, Pb^{+2}, and F^{-1} onto MOSB as adsorbent

Metal ion	Langmuir equation			Freundlich equation		
	Q_{max}	K_L	R^2	n	K_F	R^2
Cu^{+2}	12.59	0.563	0.9963	2.85	4.05	0.847
Ni^{+2}	8.19	0.227	0.976	2.75	2.02	0.86
Mn^{+2}	8.37	0.255	0.935	2.83	2.19	0.708
Pb^{+2}	12.91	0.83	0.992	3.31	4.91	0.825
F^{-1}	12.98	0.51	0.996	2.71	3.95	0.847

3.4. Adsorption Kinetics

The influence of contact time on the adsorption of Cu^{2+}, Ni^{2+}, Mn^{2+}, pb^{2+} and F^{-1} ions onto the surface of MOSB was demonstrated in Figures (12a, b) to (16a, b). The maximum removal efficiency (96, 77, 82, 97, and 95 %) for (Cu^{2+}, Ni^{2+}, Mn^{2+}, pb^{2+} and F^-) on MOSB were recorded at contact times of 90 minutes, respectively. There was no significant change after that, so the optimum contact time is 90 minutes.

Table 2 shows all the kinetic parameters of the two models at different contact time of adsorbate solution. From the table (2), it observed that the values of R^2 and $\mathbf{q_e}$ of the pseudo-second-order kinetic model were better than the pseudo-first-order kinetic model for all elements absorbed in surface of MOSB at optimum conditions. Therefore, it is more applicable to the kinetics adsorption of (Cu^{2+}, Ni^{2+}, Mn^{2+}, pb^{2+} and F^-) ions and therefore suggests a chemisorption process and the reactions are follows the second order reaction.

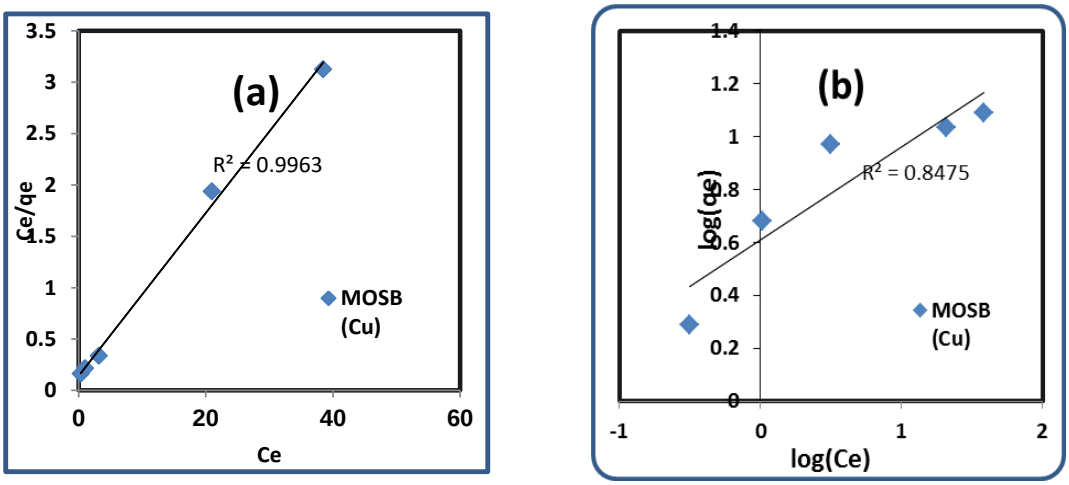

Fig. (7). Langmuir (a) and isotherm Freundlich (b) models for the adsorption of Cu^{+2} ions on to MOSB as adsorbent.

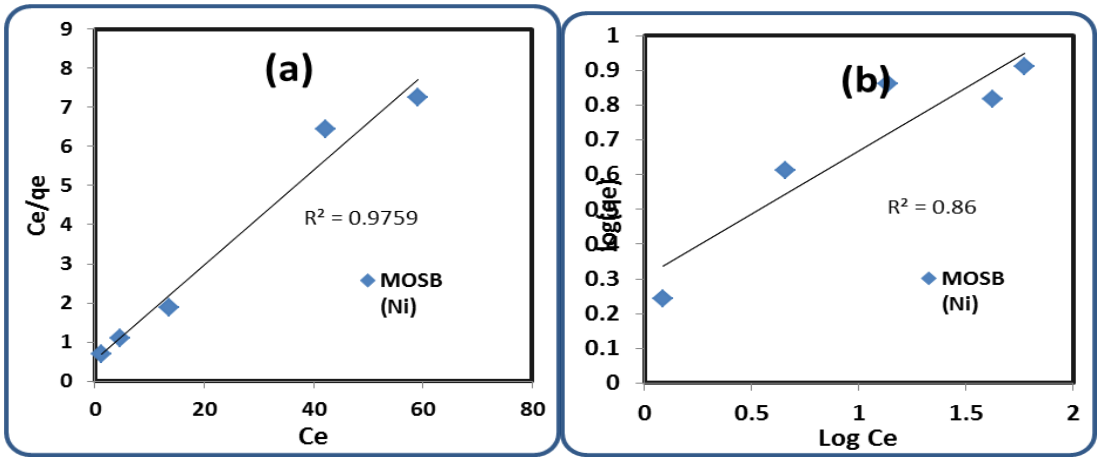

Fig. (8). Langmuir (a) and Freundlich (b) isotherm models for the adsorption of Ni^{+2}ions on to MOSB as adsorbent.

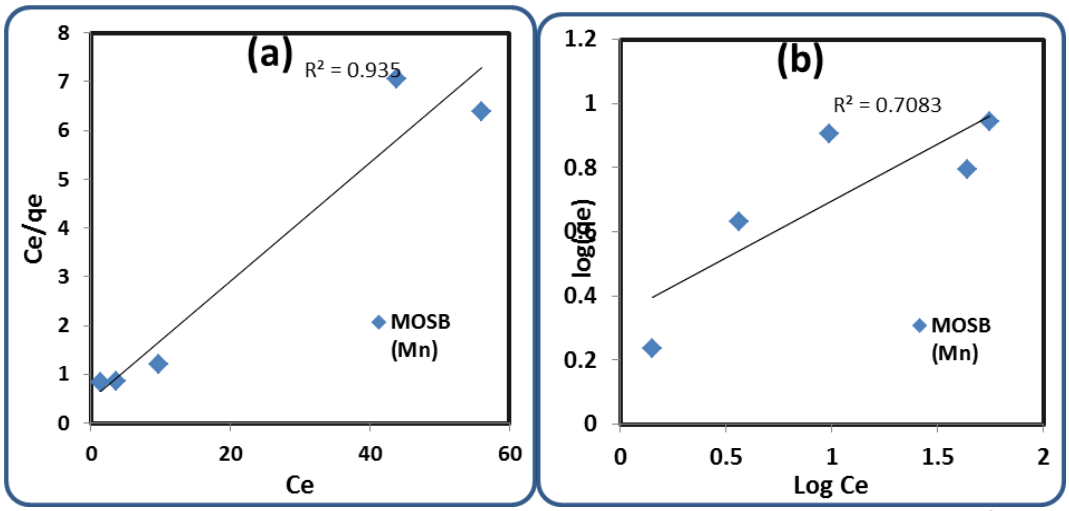

Fig. (9). Langmuir (a) and Freundlich (b) isotherm models for the adsorption of Mn^{+2} ions onto MOSB as adsorbent.

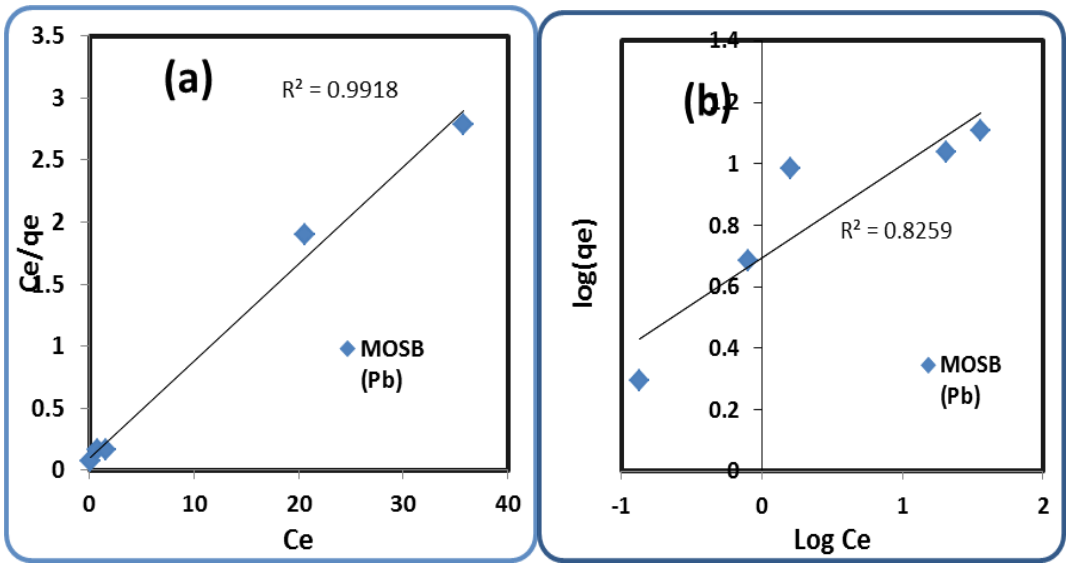

Fig. (10). Langmuir (a) and Freundlich (b) isotherm models for the adsorption of Pb^{+2} ions onto MOSB as adsorbent.

Table 2. Illustrates the Pseduo-first order and Pseduo-second order of kinetic models for the adsorption of Cu^{+2}, Ni^{+2}, Mn^{+2}, Pb^{+2}, and F^{-1} onto MOSB as adsorbent

Metal ion	Pseduo-first-order			Pseduo-second-order		
	qe	k1	R^2	qe	k2	R^2
Cu^{+2}	2.26	0.0054	0.834	9.823	0.011	0.9998
Ni^{+2}	1.805	0.0067	0.847	7.628	0.0143	0.995
Mn^{+2}	1.691	0.0052	0.742	8.439	0.0126	0.9996
Pb^{+2}	2.382	0.0058	0.74	10.183	0.0082	0.992
F^{-1}	2.035	0.005	0.787	9.7	0.01304	0.9995

3.5. Re-usability study

The capacity of the sorbent for reuse decreases until it became constant at a particular percentage of removal. The data shows only one time reuse for the adsorbent as shown in Table 3 and Figs. (17).The amount of metal removed and the number of times used depended on the heavy metal. Thus, it was determined that the sorbent may be used several times. The bio-sorption process was carried out at optimum conditions for 3hours.Table 3 and Fig. (17). illustrated the effect of bio-sorption process of the re-used MOSB after acid treatment for maximum metal ion removal at constant dose 5g/l, initial concentration 50 ppm, constant pH {(5-5.5 for metal ions) (2 for F^-)} and mixing rate 160 rpm for 90 min. it showed that; at optimum conditions of MOSB for maximum metal ions removal occurred at constant dose (5g/l).

Table 3. Illustrate the re-usability effect of MOSB after acid treatment for maximum metal ion removal at constant dose 5 g/l, initial concentration 50 ppm, constant pH (5-5.5 for metal ions and 2 for F^-)}and mixing rate 160 rpm for 90 min.

Adsorbent matter	Cu^{2+}	Ni^{2+}	Mn^{2+}	Pb^{2+}	F^{-1}
MOSB	91.31	69.21	77.18	94.41	91.73

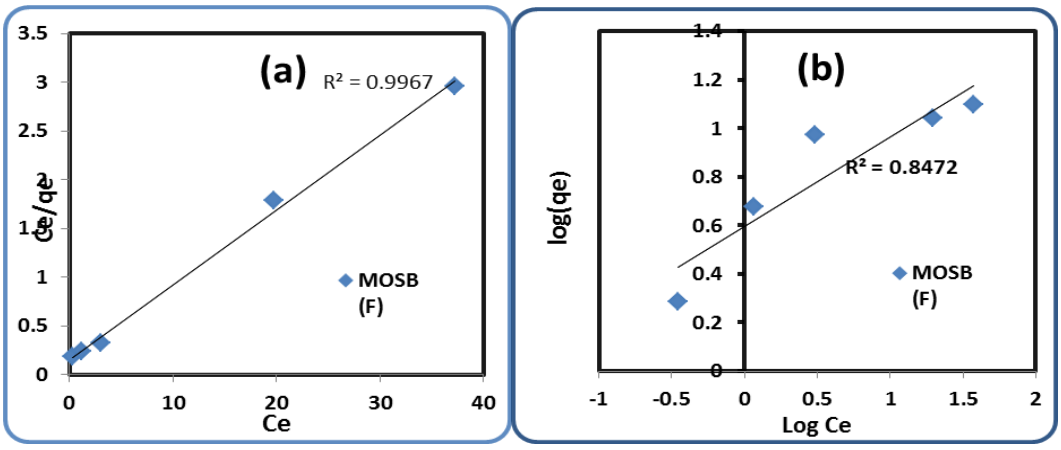

Fig. (11). Langmuir (a) and Freundlich (b) isotherm models for the adsorption of F^{-1} ions onto MOSB adsorbent.

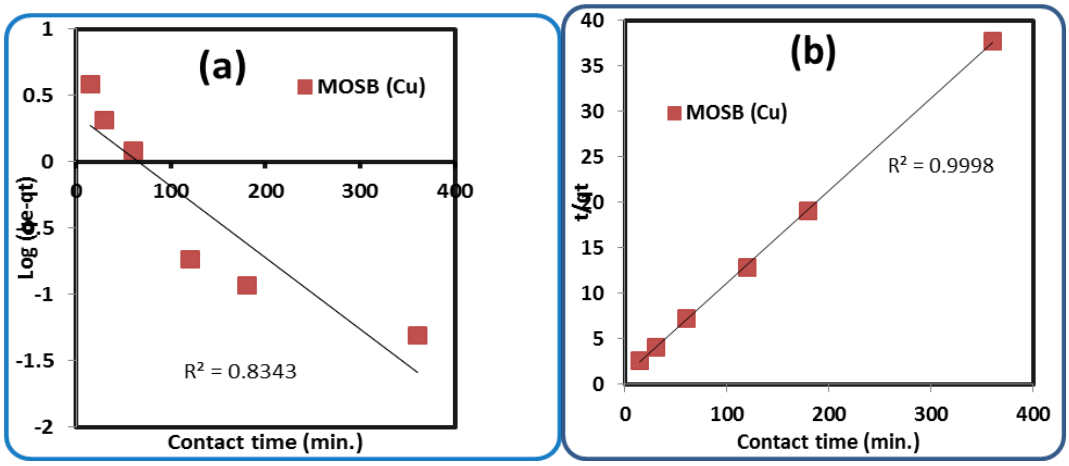

Fig. (12). Pseduo-first order (a) and Pseduo-second order (b) of kinetic models for the adsorption of Cu^{+2}ions onto MOSB adsorbent.

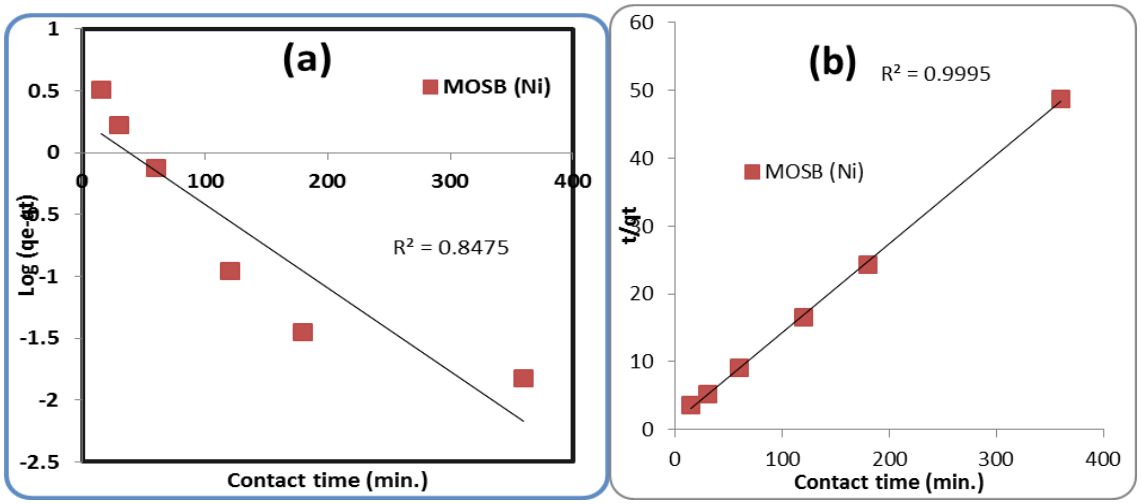

Fig. (13). Pseduo-first order (a) and Pseduo-second order (b) of kinetic models for the adsorption of Ni^{+2} ions onto MOSB adsorbent.

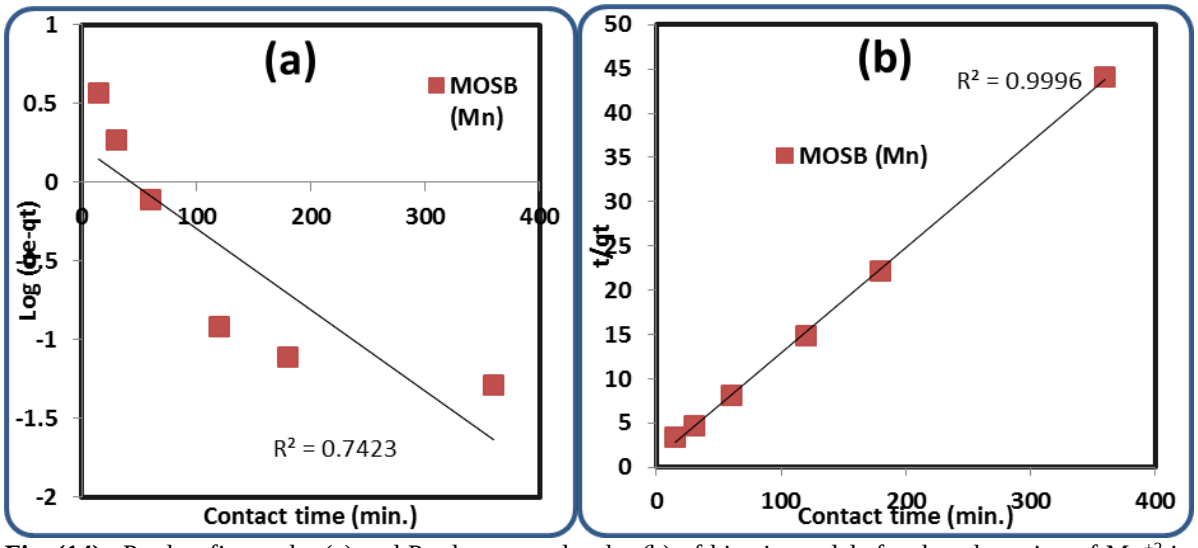

Fig. (14). Pseduo-first order (a) and Pseduo-second order (b) of kinetic models for the adsorption of Mn^{+2} ions onto MOSB adsorbent.

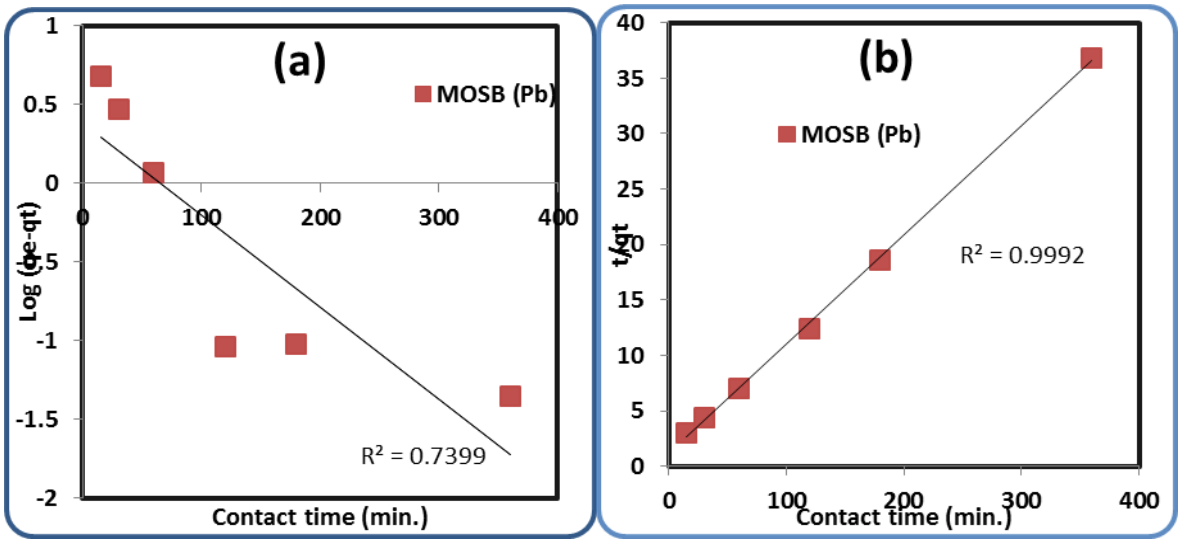

Fig. (15). Pseduo-first order (a) and Pseduo-second order (b) of kinetic models for the adsorption of Pb^{+2} ions onto MOSB adsorbent.

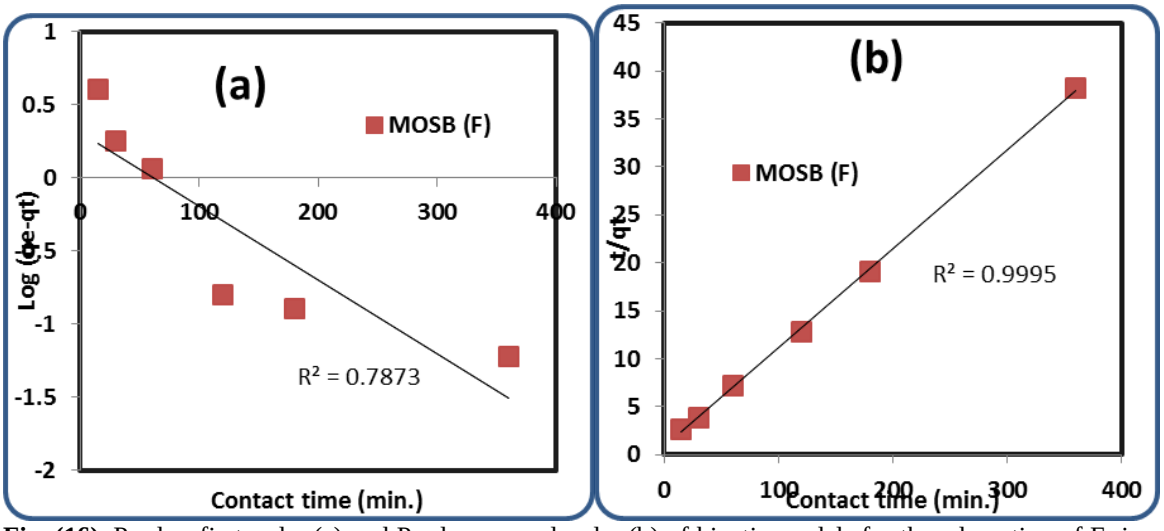

Fig. (16). Pseduo-first order (a) and Pseduo-second order (b) of kinetic models for the adsorption of F^- ions onto MOSB as adsorbent.

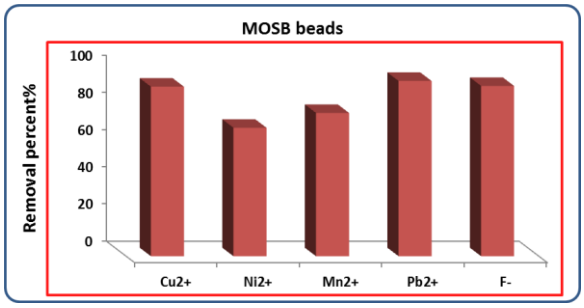

Fig. (17). Re-usability effect of MOSB after acid treatment l for maximum metal ions and fluoride removal at (T= 25°C, dose = 5 g/l, t = 60 min and (pH 5-5.5 for metal ions and pH=2 for F^{-1}).

4. CONCLUSION

Moringa seed beads (MOSB) are effective for removing heavy metals and fluoride from a simulated synthetic aqueous solution. MOSB is legitimate, cheaper, more affordable, and easier and simpler to utilize than other materials such as activated carbon. It can also be used for various useful uses and has a strong ability to adsorb heavy metal ions. It can also be reused numerous times without the requirement for a costly regeneration technique. The maximum removal efficiency of heavy metal and fluoride ion were at optimum conditions with removal efficiency (93, 72, 80, 96 and 93%) for (Cu^{2+}, Ni^{2+}, Mn^{2+}, pb^{2+} and F^{-1}) to MOSB respectively. The % elimination of heavy metal and fluoride ions were increased with increasing the adsorbent dose of bio-sorbent material, initial concentration of heavy metal and fluoride ions, and the contact time at constant mixing rate 160 rpm for both adsorbent materials. For the pH, the percentage removal metal ions was increased with increasing pH for Cu^{2+}, Ni^{2+}, Mn^{2+} and pb^{2+} while For the pH, the percentage removal of F^{-1} ions was decreased with increasing pH of solutions.

REFERENCES

[1] Reddy DH K, Seshaiah K, Reddy AVR, Rao M M, Wang MC. Biosorption of Pb^{2+} from aqueous solutions by Moringa oleifera bark: equilibrium and kinetic studies. Journal of Hazardous Materials.2010; 174(1-3): 831-8.

[2] Junior ACG, Selzlein C, Nacke H. Uso de biomassa seca de aguapé (Eichornia crassipes) visando à remoção de metais pesados de soluções contaminadas. Acta ScientiarumTechnology. 2009; 31(1):103-8.

[3] Nieto LM, Alami SBD, Hodaifa G, Faur C, Rodríguez S, Giménez JA, Ochando J. Adsorption of iron on crude olive stones. Ind Crops Prod. 2010; 32(3): 467-71.

[4] Muharrem I NCE, Ince OK. An overview of adsorption technique for heavy metal removal from water/wastewater: a critical review. Int J Pure Appl Sci.2017; 3(2): 10-9.

[5] Santos VD, Tarley CRT, Caetano J, Dragunski DC. Assessment of chemically modified sugarcane bagasse for lead adsorption from aqueous medium. Water Sci. Technol. 2010; 62(2): 457-65.

[6] Dos Santos VC, De Souza JV, Tarley CR, Caetano J, Dragunski DC. Copper ions adsorption from aqueous medium using the biosorbent sugarcane bagasse in natural and

chemically modified. Water, Air, Soil Pollut. 2010; 216(1): 351-59.

[7] Peña-Rodríguez S, Fernández-Calviño D, Nóvoa-Muñoz JC , Arias-Estévez M, Núñez-Delgado A, Fernández-Sanjurjo MJ, Álvarez-Rodríguez E. Kinetics of Hg (II) adsorption and desorption in calcined mussel shells. J Hazard Mater.2010; 180(1-3): 622-27.

[8] Gupta VK, Ali I. Utilisation of bagasse fly ash (a sugar industry waste) for the removal of copper and zinc from wastewater. Sep Purif Technol.2000; 18(2): 131-40.

[9] Han X, Liang CF, Li TQ, Wang K, Huang HG, Yang XE. Simultaneous removal of cadmium and sulfamethoxazole from aqueous solution by rice straw biochar. J Zhejiang Univ Sci. 2013; 14(7): 640-49.

[10] Memon JR, Memon SQ, Bhanger MI, Memon GZ, El-Turki A, Allen GC. Characterization of banana peel by scanning electron microscopy and FT-IR spectroscopy and its use for cadmium removal. Colloids Surf. B. 2008; 66(2): 260-65.

[11] Bilal M, Shah JA, Ashfaq T, Gardazi SMH, Tahir AA, Pervez A, Mahmood Q. Waste biomass adsorbents for copper removal from industrial wastewater—a review. J Hazard Mater.2013; 263(2): 322-33.

[12] Al Bsoul A, Zeatoun LY, Abdelhay A, Chiha M. Adsorption of copper ions from water by different types of natural seed materials. Desalination water Treat. 2014; 52(31-33): 5876-82.

[13] Ongulu RA. Biosorption of Pb^{2+} and Cr^{2+} using Moringa oleifera and their adsorption isotherms. Sci J Anal Chem. 2015; 3(6):100-8.

[14] Ghafar F, Mohtar A, Sapawe N, Hadi NN, Salleh MRM. Chemically modified Moringa oleifera seed husks as low cost adsorbent for removal of copper from aqueous solution. AIP Conference Proceedings, AIP Publishing LLC.2017; 1901(1): 100002.

[15] Ali EN, Seng HT. Heavy metals (Fe, Cu, and Cr) removal from wastewater by Moringa oleifera press cake. MATEC Web of Conferences.2018; 150: 02008.

[16] Aziz NAA, Jayasuriya N, Fan L. Adsorption study on Moringa oleifera seeds and Musa 38odeling38 as natural water purification agents for removal of Lead, Nickel and Cadmium from drinking water. IOP Conference Series: Materials Science and Engineering. 2016;136(1): 012044).

[17] Aziz NAA, Jayasuriya N, Fan L. Adsorption study on Moringa oleifera seeds and Musa Cavendish as natural water purification agents for removal of Lead, Nickel and Cadmium from drinking water. IOP Conference Series Mat Sci Eng. 2016; 136(1): 012044.

[18] Taha GM, Ibrahim NH. Moringa-TiO_2 nano composite (MT_2) for removal of methylene blue (MB) and methyl orange (MO) dyes from their aqueous solutions. Al-Azhar Bulletin of Science. 2019; 30(1-A (Chemistry)): 91-103.

[19] Langmuir I. The adsorption of gases on plane surfaces of glass, mica and platinum. J Am Chem Soc 1918; 40(9):1361–03.

[20] Lagergren S. About the theory of so-called adsorption of soluble substances. Handlingar Band.1898; 24:1-39.

[21] Ho YS. Removal of copper from aqueous solution by aminated and protonated mesoporous aluminas: kinetics and equilibrium. Journal of colloid and interface science.2004;276(1): 255-58.

[22] Reddy DHK, Seshaiah K, Reddy AVR, Lee SM . Optimization of Cd (II), Cu (II) and Ni (II) biosorption by chemically modified Moringa oleifera leaves powder. Carbohydrate Polymers. 2012; 88(3): 1077-86.

[23] Swelam AA, Sherif SS, Ibrahim A. The adsorption kinetics and modeling for Pb (II) removal from synthetic and real wastewater by moringa oleifera seeds. Al-Azhar Bulletin of Science. 2018; 29(2-A): 105-24.

[24] Bhutada PR, Jadhav AJ, Pinjari DV, Nemade PR, Jain RD. Solvent assisted extraction of oil from Moringa oleifera Lam. Seeds. Ind. Crops prod. 2016; 82: 74-80.

[25] Pagnanelli F, Mainelli S, Vegliò F, Toro L. Heavy metal removal by olive pomace: biosorbent characterisation and equilibrium modeling. Chem. Eng. Sci. 2003; 58(20): 4709-17.

[26] Farhaoui M, Derraz M. Optimizing coagulation process by using sludge produced in the water treatment plant. J Chem Pharm Res. 2016; 8(4): 749-56.

[27] Farhaoui M, Hasnaoui L, Derraz M. Optimization of drinking water treatment process by modeling the aluminum sulfate dose. Br J Appl Sci Technol.2016; 17(1): 1-14.

[28] Selvi K, Pattabhi S, Kadirvelu K. Removal of Cr (VI) from aqueous solution by adsorption onto activated carbon. Bioresour Technol. 2001; 80(1): 87-9.

[29] Merzouk B, Gourich B, Madani K, Vial C, Sekki A. Removal of a disperse red dye from synthetic wastewater by chemical coagulation and continuous electrocoagulation. A comparative study. Desalination. 2011; 272(1-3): 246-53.

إزالة المعادن الثقيلة والفلوريد من المياه الملوثة باستخدام خرز بذور المورنجا

خالد م. خضر [1] ، ربيع س. فرج [1]، مصطفى م. أبو الفضل [2] ، محمد علي [2]

1. قسم الكيمياء ، كلية العلوم (بنين) ، جامعة الأزهر ، القاهرة ، مصر.

2. مركز بحوث الصحراء ، القاهرة ، مصر.

الملخص:

تلوث المياه بالمعادن الثقيلة له عواقب صحية ضارة وخطيرة على الإنسان، والهدف من هذه الدراسة هو معرفة مدى فعالية حبات بذور المورينجا الممزوجة بألجينات الصوديوم (MOSB) في امتصاص الأيونات مثل النحاس والنيكل والمنغنيز والرصاص والفلورايد من المياه الملوثة وتم استخدام طرق مفيدة مختلفة لوصف الممتزات (FT-IR) و(SEM) تم تحسين دراسات الامتزاز الدفعي وتأثيرات معاملات الامتزاز. أظهرت النتائج أن معدل الإزالة لكل عنصر حدث عند الجرعة المثلى (5 جم / لتر) بكفاءة الإزالة (93 ، 72 ، 80 ، 96 ، 93٪) وقدرة امتصاص قصوى (.Qmax) حوالي (12.5). ، 8 ، 8.3 ، 13 ، 13 مجم / جم) للنحاس والنيكل والمنغنيز وأيونات الرصاص والفلورايد ، على التوالي. كان لكل من الأس الهيدروجيني ، وجرعة التخثر ، والخلط ، والتركيز ، والعكارة الأولية للماء تأثير على إزالة المعادن الثقيلة وأيونات الفلوريد. في الختام ، يمكن اعتبار MOSB مادة بديلة مستدامة لأنها غير مكلفة ، ولا تتطلب معالجة مسبقة ، وهي ماصة بيولوجية لإزالة المعادن الثقيلة وأيونات الفلوريد من مياه الصرف الصحي.